JOURNAL OF CATALYSIS 59, 223–238 (1979)

# Reduction of NO by CO over a Silica-Supported Platinum Catalyst: Infrared and Kinetic Studies

D'ARCY LORIMER[1] AND ALEXIS T. BELL

*Department of Chemical Engineering, University of California, Berkeley, California 94720*

Received December 14, 1978; revised February 26, 1979

The reduction of NO by CO was studied over a $Pt/SiO_2$ catalyst at 300°C. Reaction rate data were obtained together with *in situ* infrared spectra of species adsorbed on the catalyst surface. The performance of the catalyst depended strongly on the ratio of CO/NO in the reactor. For net reducing conditions (CO/NO > 1) the catalyst deactivated with time. Measurements of kinetics taken during a period of slow deactivation showed that the rate of NO reduction was first order in NO and inverse second order in CO. Reactivation of the catalyst was obtained with both oxidizing and reducing pretreatments. Under net oxidizing conditions (CO/NO < 1) the catalyst was much more active than under reducing conditions and did not deactivate. *In situ* infrared spectra showed bands corresponding to CO chemisorbed on Pt and NCO and CN groups attached to the support as Si–NCO and Si–CN, respectively. Both the CO and NCO bands were more intense under reducing than oxidizing conditions. The kinetics and product selectivities observed under reducing conditions were found to be in good agreement with a mechanism based upon the dissociation of NO as the rate-limiting step. This mechanism further assumes that $N_2O$ is formed by reaction of adsorbed NO with an adsorbed nitrogen atom. It is proposed that the loss in catalyst activity is associated with a change in the electronic properties of the supported Pt crystallites, caused by the accumulation of large concentrations of NCO and CN groups on the support in areas adjacent to the crystallites.

## INTRODUCTION

The reduction of NO by CO over supported Pt catalysts has been investigated (*1–6*) as part of the effort to find suitable catalysts for abatement of automotive NO emissions. While the activity of Pt relative to other transition metals and the response of the reduction rate to reaction conditions have been established, there have been few investigations of reaction mechanism and kinetics. Based upon studies of the reactions between NO and CO coadsorbed on Pt (111) and (110) surfaces, Lambert and Comrie (*7*) proposed that the dissociation of NO is the rate-limiting step. Nitrogen was shown to be formed by the recombination of adsorbed nitrogen atoms and $N_2O$ by the reaction of adsorbed NO and adsorbed atomic nitrogen. The kinetics of NO reduction by CO over a $Pt/SiO_2$ catalyst were studied by Cant *et al.* (*8*). The NO reaction rate was determined to be approximately first order in NO partial pressure and approached inverse first order in CO partial pressure. The authors suggested that these kinetics were consistent with the mechanism proposed by Lambert

[1] Present address: Western Electric Co., P.O. Box 900, Princeton, N.J. 08540.



0021-9517/79/110223-16$02.00/0

and Comrie (*7*) and supported the idea that $N_2O$ is formed via a Langmuir–Hinshelwood mechanism.

Infrared investigations of the interactions between NO and CO on Pt catalysts have shown that an isocyanate species is formed (*9–16*). While it was originally thought that this species was present on the metal surface, more recent studies clearly indicate that it resides on the support (*13–15*). A clear mechanistic role for the isocyanate structure has not been established. However, Niiyama *et al.* (16) have observed that the growth of an intense isocyanate band parallels the deactivation of a Pt/$Al_2O_3$ catalyst. The authors concluded that the loss in activity was probably due to a reduction in metal surface area caused by the accumulation of Pt–NCO groups.

The present investigation was undertaken to study the mechanism and kinetics of NO reduction by CO over Pt further, with particular emphasis being given to determining the effects of gas composition on the kinetics of NO reduction and product composition. *In situ* infrared observations were used to identify adsorbed molecular species on the catalyst surface. Based upon this information it was possible to establish more clearly the effects of isocyanate species on catalyst activity.

## EXPERIMENTAL METHODS

*Apparatus.* The apparatus used to obtain the spectral and kinetic data reported here has been described previously (*17*). The reactor is a heated infrared cell made of 316 and 304 stainless steel. A catalyst disk was held within the reactor so that it was aligned with the sample beam of the infrared spectrometer (Perkin–Elmer 457). A second disk, consisting of the catalyst support, was held in the reference beam. Using this technique it was possible to subtract out the spectrum of the support and of species present in the gas phase. To accommodate additional catalyst within the reactor, a circular catalyst holder was located midway between the two disks used for infrared investigations. The bed of catalyst in the holder was 25 mm in diameter and 6 mm deep. The catalyst was contained by Fiberglas cloth stretched across the circular faces of the bed. Calculations indicated that transport into the bed was not diffusion limited until a conversion substantially greater than 99% was achieved.

Initial experiments revealed that the walls and internals of the reactor had sufficient catalytic activity to pose a problem. To minimize this, the surfaces exposed to the hot reactants were coated with a noncatalytic material by means of the following procedure. The stainless-steel surfaces were first cleaned and then nickel plated to help smooth any surface roughness. A 2000-Å aluminum coating was next applied by ion plating. To prevent diffusion of this layer into the steel and the outward diffusion of elements from the steel, the aluminum coating was oxidized. Next, a second 2000-Å-thick coating was applied over the oxide layer. Finally, the reactor and internal parts were placed in an air oven at 400°C for 200 hr to grow a dense $\gamma$-$Al_2O_3$ crystalline film (*18*).

The alumina coating reduced the background activity to a tolerable level (viz. $<10\%$ of the catalyst activity). However, with repeated use of the reactor the effectiveness of the coating decreased. To overcome this problem, the reactor walls and the catalyst holder were coated with a thin layer of Vacseal (Space Environmental Labs), a silicone-based material developed for the repair of leaks in ultrahigh vacuum chambers. The Vacseal provided a transparent coating which was stable to repeated heating up to 350°C in both oxidizing and reducing environments. The coated reactor could be evacuated to $10^{-6}$ Torr at 300°C and showed no evidence of degassing. Properly cured, the Vacseal coating reduced the background activity

down to the level originally attained with the freshly deposited alumina coating.

The reactor was connected to a gas recycle loop containing two preheaters upstream of the reactor and a forced air-cooled coil downstream of the reactor. To minimize background activity, both the preheater and cooling coil were made of aluminum tubing (alloy T6061). Gas flow in the loop was provided by a 40 liter/min stainless-steel bellows pump. Reactants were continually fed into, and products were withdrawn from, the recirculating gases. With a nominal flow rate of 200 $cm^3$/min to the loop, a recycle ratio of 200:1 could be achieved, allowing the reactor to be characterized as a CSTR.

Analysis of the products was accomplished using two gas chromatographs connected in series. The first chromatograph contained a 3-m-long 6-mm-o.d. column packed with Porapak R, which was maintained at 100°C. This column separated $N_2O$ and $CO_2$ but passed through NO, CO, and $N_2$ as a single unresolved peak. This peak was resolved in the second chromatograph which contained a 3-m-long 6-mm-o.d. column packed with 5-Å molecular sieves, which was maintained at 90°C. Valving between the two chromatographs prevented the $CO_2$ and $N_2O$ eluted from the first column from entering the second.

*Materials.* A 4.5% $Pt/SiO_2$ catalyst was prepared by platinum amine ion exchange (*19*, *20*). Two types of silica were used as supports, Davidson 70 silica gel (−80 + 150 mesh) and Cabot Hs-5 Cab-O-Sil. The ion exchanged silica was freeze dried and then reduced in flowing hydrogen for 3 hr at 400°C. The Pt surface area of the reduced catalyst was determined by $H_2$ chemisorption. Monolayer coverage was found to be 100 μmole/g for the catalyst supported on silica gel and 106 μmole/g for the catalyst supported on Cab-O-Sil, corresponding to Pt dispersion of 91 and 90%, respectively.

Preliminary experiments revealed that the catalyst activity and the infrared spectra of adsorbed species were independent of the type of support used but that superior infrared samples could be prepared using the Cab-O-Sil-supported material. At the same time it was established that the silica gel-supported material could more easily be retained in the central catalyst holder because of the larger particle size of the support (−80 + 150 mesh). Accordingly, 1 g of the silica gel-supported catalyst was placed in the central holder and 160 mg of the Cab-O-Sil-supported catalyst was pressed a 25-mm disk and used for infrared observations.

Helium (99.998%) and $H_2$ (99.999%) were used without further purification. Nitric oxide (99.0%) was passed through a dry ice–acetone trap to remove $N_2O$, one of the major impurities. No attempt was made to separate $N_2$, the other major impurity, from NO. Carbon monoxide (99.9%) was passed through a molecular seive trap cooled in a dry ice–acetone bath to remove traces of iron carbonyls.

*Experimental procedure.* The procedure for each experiment was essentially the same. The reactor was first heated to 300°C while purging it with flowing He. Next, the catalyst was oxidized for 2 hr at 300°C in a flow of 20% $O_2$ in He and then reduced for 5 hr at 300°C in flowing $H_2$. The reactor was then purged of $H_2$ with a flow of He. At this point a premixed feed of NO and CO in He was introduced into the reactor. The product composition was then analyzed periodically, over a 3-hr period. At the end of the experiment the feed flow was discontinued and the reactor was purged with He. Prior to beginning a new experiment the catalyst was again oxidized and reduced.

## RESULTS

### *Kinetics*

Reaction kinetics were investigated at 300°C over a range of NO and CO partial

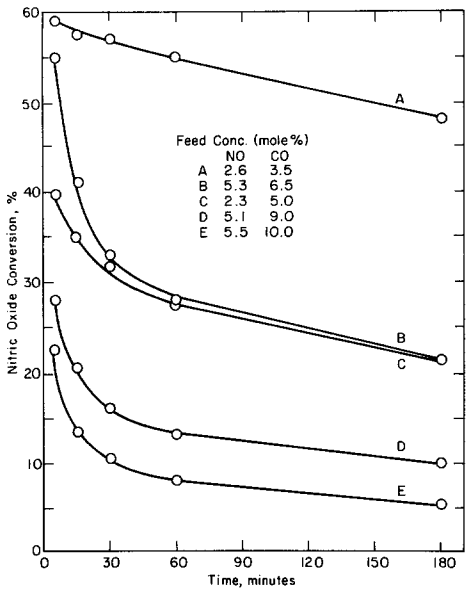


FIG. 1. NO conversion versus time for runs made under reducing conditions.

pressures. At the outset of these studies it was observed that the catalyst activity and stability depended very strongly upon the feed ratio of CO/NO. Correspondingly, the results have been organized into two groups, those taken with CO/NO ratios greater than one, designated as reducing conditions, and those taken with CO/NO ratios less than one, designated as oxidizing conditions.

The conversion of NO as a function of time is shown in Fig. 1 for runs made under reducing conditions. For each feed mixture the catalyst exhibits a loss in activity with time. Both the initial NO conversion and the extent of deactivation depend upon the feed composition in a similar fashion. The highest initial activity and lowest degree of deactivation are realized for low-feed concentrations of both reactants and ratios of CO/NO close to unity.

The loss in catalyst activity observed at the end of a 3-hr run could be fully restored by the standard oxidation/reduction pretreatment. To investigate the origins of the deactivation process further a series of runs were made in which the catalyst was first exposed to either oxidizing or reducing conditions prior to introduction of a feed mixture containing 10% CO and 5% NO. Preoxidation was carried out for 5 hr at 300°C with a 5% NO in He mixture, and prereduction was carried out for 2 hr at 300°C in a 10% CO in He mixture. The results of pretreatment with NO and CO are shown in Fig. 2 and compared with the results for a standard pretreatment. It is apparent that initial exposure to either NO or CO does not cause a substantial change in the initial NO conversion or the subsequent pattern of deactivation. The observed

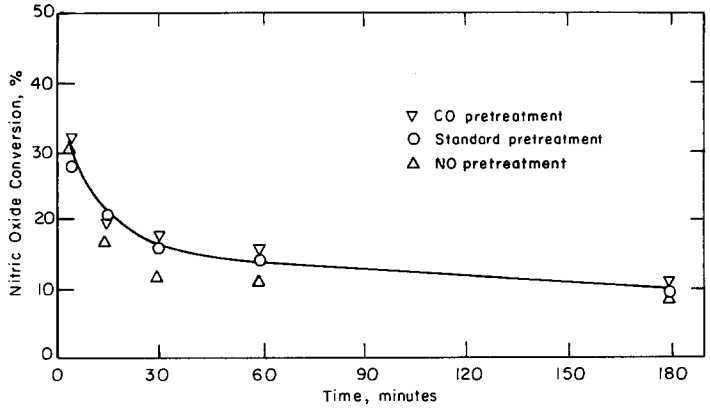


FIG. 2. Effects of catalyst pretreatment on subsequent activity.

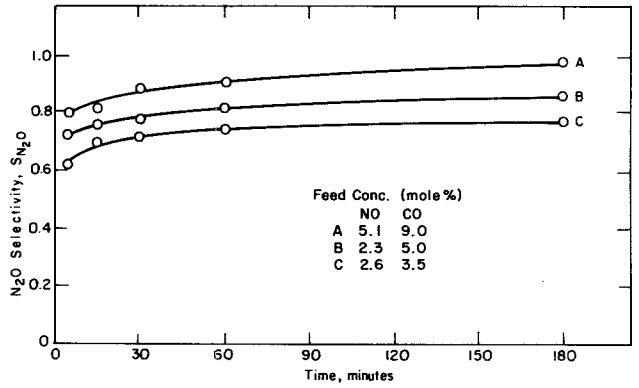


FIG. 3. $N_2O$ selectivity versus time for runs made under reducing conditions.

spread in the data at intermediate times is comparable to that noted in reproducing runs for a given set of conditions. While not shown in Fig. 2, it was also found that the initial activity could be restored by contacting the catalyst with either NO or CO alone at the end of a run.

The catalyst selectivity for $N_2O$ formation is defined by Eq. (1) and is illustrated as a function of time in Fig. 3.

$$S_{N_2O} = r_{N_2O}/(r_{N_2} + r_{N_2O}). \qquad (1)$$

For the conditions investigated, the $N_2O$ selectivity ranged between 0.6 and 0.95 and increased by roughly 20% during the course of a run.

The stoichiometric ratio of the nitrogen- and carbon-containing products was also determined. This quantity, designated as $R_s$, is defined by

$$R_s = (r_{N_2O} + 2r_{N_2})/r_{CO_2} \qquad (2)$$

and is based upon the stoichiometries of the reactions producing $N_2O$ and $N_2$ via the reduction of NO by CO. If no additional reactions occur, $R_s$ should be unity. The observation of $R_s$ values greater or less than unity indicates the occurrence of side reactions involving one or both reactants.

The behavior of $R_s$ in the reducing region is shown in Fig. 4 for two runs. The data shown define the range of observed $R_s$ values, with all other runs having values falling in the region between the two curves. In all cases $R_s$ is less than unity, but for a given run the value of $R_s$ rises slightly as the run proceeds.

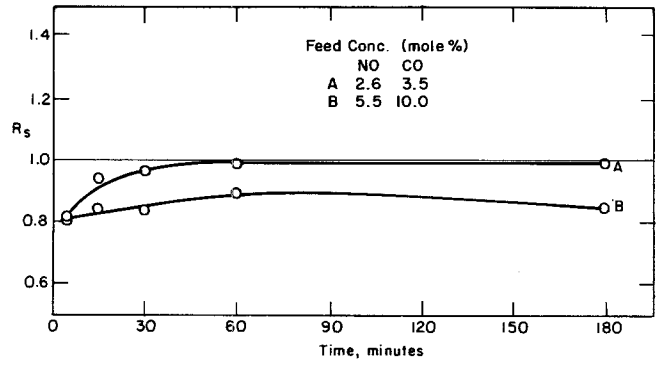


FIG. 4. $R_s$ versus time for runs made under reducing conditions.

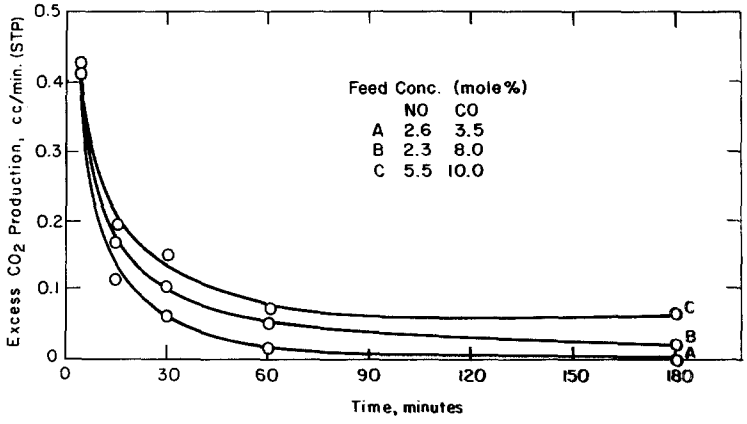


FIG. 5. Excess $CO_2$ production versus time for runs made under reducing conditions.

The lowest value of $R_s$ corresponds to the highest feed ratios of CO/NO and conversely the highest value of $R_s$ corresponds to CO/NO ratios close to unity.

The fact that $R_s$ is less than one indicates that the production of $CO_2$ is in excess of that required to stoichiometrically balance the observed $N_2$ and $N_2O$. Figure 5 illustrates how the rate of excess $CO_2$ production changes with time. Initially the rate decreases sharply. This is followed by a more gradual decrease over a more extended period of time. Consistent with the trends in $R_s$, the highest rates of excess $CO_2$ production are found for runs made under highly reducing conditions.

The reaction kinetics under oxidizing conditions are distinctly different from those observed under reducing conditions. The conversion, based upon CO, is always very high, falling in the range of 0.95 to ~1.0. In contrast to the behavior observed under reducing conditions, the catalyst activity rises slightly and then remains constant for an extended period of time as shown in Fig. 6.

Nitrous oxide selectivities for four typical runs are shown in Fig. 7. The lowest selectivities are found for runs in which the CO/NO feed ratio is close to unity. With increasing NO content in the feed the $N_2O$ selectivity increases. It should be recognized that because of the high CO conversions, the actual ratio of CO/NO

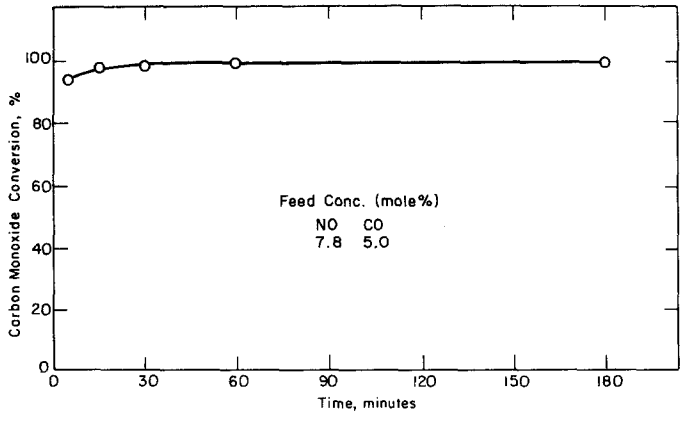


FIG. 6. NO conversion versus time for a run made under oxidizing conditions.

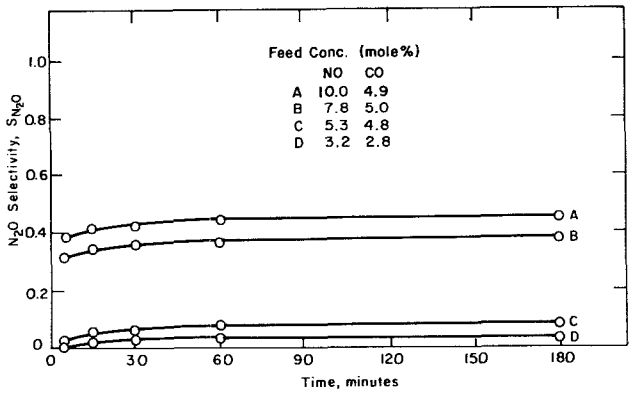


FIG. 7. $N_2O$ selectivity versus time for runs made under oxidizing conditions.

over the catalyst is much lower than that in the feed.

A further contrast between catalyst behavior under oxidizing versus reducing conditions, is shown in Fig. 8. The curve of $R_s$ as a function of time is typical of reaction in the presence of excess NO. The value of $R_s$ is slightly greater than unity and remains essentially constant over the duration of the run.

*Infrared Spectra*

Typical double beam spectra taken under reducing and oxidizing conditions are shown in Fig. 9. Two strong bands appear at 2075 and 2280 $cm^{-1}$ and a weaker band is seen at 2190 $cm^{-1}$. A single beam spectrum of the catalyst disk shows the same features but the 2280 $cm^{-1}$ band is centered at 2320 $cm^{-1}$, and a weaker but well-defined band appears at 2350 $cm^{-1}$. As is discussed below, the difference in positions of the band near 2300 $cm^{-1}$, when observed in single and double beam modes, is due to the presence of a comparable band on the support. Thus, in the double beam mode the spectrum recorded is the difference between the spectra of the catalyst and reference disks.

The band at 2075 $cm^{-1}$ can readily be assigned to CO chemisorbed on Pt (*21*, *22*). The two bands at 2350 and 2320 $cm^{-1}$ are in good correspondence with absorbances observed for isocyanate (NCO) groups on the surface of silica attached as Si–NCO (*13*, *14*, *23*, *24*). Accordingly, the band ob-

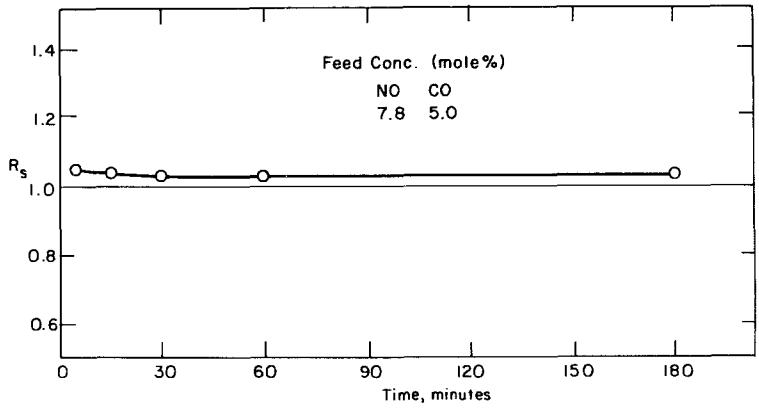


FIG. 8. $R_s$ versus time for a run made under oxidizing conditions.

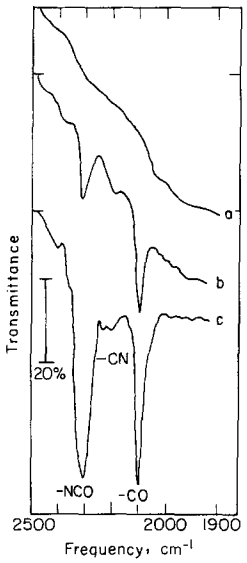


FIG. 9. Representative infrared spectra: (a) background; (b) $T = 300°C$, $P_{NO} = 0.10$ atm, $P_{CO} = 0.05$ atm; (c) $T = 300°C$, $P_{NO} = 0.05$ atm, $P_{CO} = 0.10$ atm.

served at 2280 $cm^{-1}$ in the double beam spectra is also assigned to Si–NCO. The remaining band at 2190 $cm^{-1}$ is assigned to cyanide (CN) groups present on the silica surface as Si–CN (*23*, *24*). The absence of bands in the region between 1760 and 1785 $cm^{-1}$, either under reducing or oxidizing conditions, suggests that coverage of the surface by chemisorbed NO is very small (*22*, *25*).

Under reducing conditions the CO band intensity achieved its final value immediately upon the introduction of the reactants. The position of the band was independent of gas composition, but the absorbance varied between 0.3 and 0.4 as the concentration of CO in the gas over the catalyst varied from 2 to 8%. As a point of reference it was established that an absorbance of 0.4 corresponded to saturation coverage by CO at 300°C.

The formation and growth of the NCO and CN bands were time dependent and complex. On a fresh catalyst disk, most of the NCO band growth took place during the first 30 to 60 min of exposure to the reactants. Once formed, the NCO band was very stable and could not be removed by prolonged heating in He at 300°C or by the standard pretreatment process. Because of this stability, repeated runs made under reducing conditions induced additional band growth as shown in Fig. 10. Notice that as the NCO band becomes very intense, it appears to resolve into two bands centered at 2300 and 2250 $cm^{-1}$. With repeated use and reactivation of the catalyst, the NCO bands appear to attain a maximum intensity but the CN band grows continuously. Quite interestingly, the growth of the NCO and CN bands does not influence the position or intensity of the CO band. This observation contrasts with that of Chang and Hegedus (*26*) who observed an upscale shift of the CO band frequency with the growth of NCO

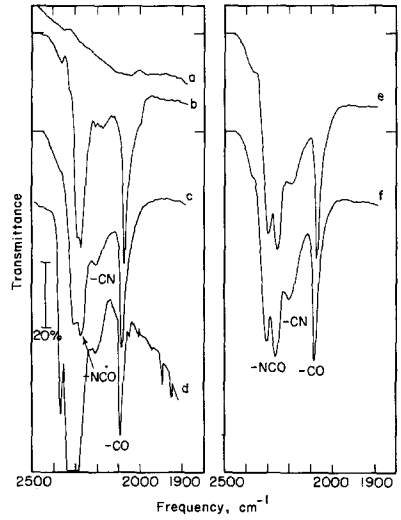


FIG. 10. Infrared spectra showing the effects of reaction time and catalyst cycling: (a) background; (b) $T = 300°C$, $P_{NO} = 0.05$ atm, $P_{CO} = 0.10$ atm spectrum after 30 min of reaction; (c) spectrum after 150 min of reaction; (d) some spectrum as b but taken in single beam mode; (e) spectrum after 150 min of reaction following standard catalyst pretreatment and recontacting with the feed composition indicated for spectrum b; (f) spectrum after 150 min of reaction following standard catalyst pretreatment and recontacting with the feed composition indicated for spectrum b.

bands in studies conducted over a $Pt/Al_2O_3$ catalyst.

Interpretation of the changes in the NCO band intensity seen in Fig. 10 is complicated by the fact that a spectrum of the silica disk used as a reference also shows a strong NCO band. This suggests that NCO species produced on the catalyst disk are in some fashion transferred to the reference disk through the gas phase. The presence of NCO groups on the reference disk explains why a single beam spectrum of the catalyst disk shows only a single band at 2320 $cm^{-1}$ which is much more intense than that obtained in a single beam spectrum taken with a reference disk. It also suggests that the splitting in the NCO band seen in Fig. 10 is an artifact produced by taking the difference of spectra of NCO groups present on the catalyst and reference disks.

The NCO band is easily eliminated by exposure of the catalyst to water vapor (~20% relative humidity) at 25°C. This process is illustrated in Fig. 11. It is interesting to observe that the removal of the NO band is accompanied by the growth of the CN band. This suggests that the CN species may result from NCO hydrolysis. It is also observed that the NCO species on the reference disk appears to be more resistant to removal by water at room temperature than that present on the catalyst disk, as evidence by the appearance of an inverted band at 2300 $cm^{-1}$ in spectrum d. Complete removal of all bands was obtained by heating to 300°C in He.

The infrared spectra taken under oxidizing conditions showed bands at the same frequencies as spectra recorded under reducing conditions, but the band intensities were in general smaller under oxidizing conditions (see Fig. 9). The behavior of the CO band was similar to that observed in the reducing region, i.e., the initial formation was very rapid and no time dependent growth or frequency shifts were noted. The range of absorbance varied from approximately 0.2 to 0.3, and the smallest bands were seen when the CO concentration was lowest and the NO concentration was highest. The NCO band grew with time during a run, in a manner similar to that observed under reducing conditions

## DISCUSSION

### *Kinetics*

The observed trends in reaction rate and product selectivity can be discussed in terms of the following mechanism. Reactions 1 and 2 represent

$$1.\quad CO + S \rightleftarrows CO_s$$

$$2.\quad NO + S \rightleftarrows NO_s$$

$$3.\quad NO_s + S \rightarrow N_s + O_s$$

$$4.\quad N_s + N_s \rightarrow N_2 + 2S$$

$$5a.\quad N_s + NO_s \rightarrow N_2O + 2S$$

$$5b.\quad N_s + NO \rightarrow N_2O + S$$

$$6.\quad CO + O_s \rightarrow CO_2 + S$$

the reversible chemisorption of CO and NO, respectively. The dissociation of NO is taken to occur via molecularly adsorbed NO as suggested by the work of Lambert and Comrie (*7*) and Pirug and Bonzel (*27*). Nitrogen formation is described by the recombination of adsorbed nitrogen atoms. Experimental evidence for this process has been presented by Wilf and Dawson (*28*) and Schwaha and Bechtold (*29*), as well as the previously mentioned authors (*7*, *27*). Low-pressure studies by Lambert and Comrie (*7*) and Pirug and Bonzel (*27*) have also indicated that $N_2O$ is formed by reaction 5a. The inclusion of reaction 5b is based upon the theoretical work of Weinberg and Merrill (*30*), which suggests that at moderate NO partial pressures reaction 5b should be favored over reaction 5a. The final step, reaction 6 describes the removal of adsorbed oxygen from the surface. Preference for this process over

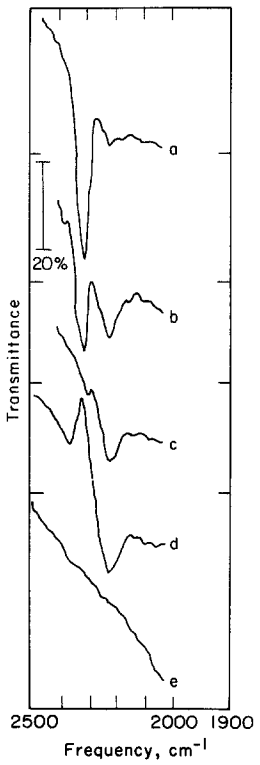


FIG. 11. Effects of water vapor on the NCO and CN bands: (a) spectrum prior to exposure to water vapor; (b) 30 min after introduction of $6 \times 10^{-3}$ atm $H_2O$ in He at 25°C; (c) 60 min after introduction of $H_2O$/He mixture; (d) 240 min after introduction of $H_2O$/He mixture; (e) after heating in He at 300°C for 120 min.

a Langmuir–Hinshelwood process involving adsorbed CO is indicated by the experimental results of Bonzel and Ku (*31*).

It should be noted that while reactions 1 through 6 provide a complete mechanism for NO reduction, no account is taken of the formation and destruction of NCO groups. This is intentional and can be justified on the basis of the following reasoning. As will be discussed below, the rate of NO consumption associated with the formation of NCO group is never greater than 10% and usually less than 5% of the total NO consumption. Furthermore, the surface coverage of Pt by NCO groups is negligible and, hence, does not affect the availability of sites for either NO or CO adsorption.

Under reducing conditions, it is assumed that the reduction of NO is rate limited by the dissociation of chemisorbed NO. The rate of NO disappearance can then be expressed as

$$r_{NO} = \frac{k_3 K_2 P_{NO}}{(1 + K_1 P_{CO} + K_2 P_{NO})^2} \qquad (3)$$

where $k_i$ and $K_i$ represent the rate coefficient and equilibrium constant for reaction $i$, respectively. In deriving Eq. (3), it is assumed that surface coverage by atomic species is considerably less than by molecular species. Since the infrared observations presented here indicate that CO chemisorbs strongly and in preference to NO, we can assume that the second term in the denominator of Eq. (1) is dominant. By this means Eq. (3) reduces to

$$r_{NO} = k P_{NO}/P_{CO}^2 \qquad (4)$$

where $k = k_3 K_2 / K_1^2$.

A plot of $r_{NO}$ versus $P_{NO}/P_{CO}^2$ is shown in Fig. 12. The data points, representing the rate of reaction 60 min into a run, are seen to scatter around a straight line passing through the origin. From the slope

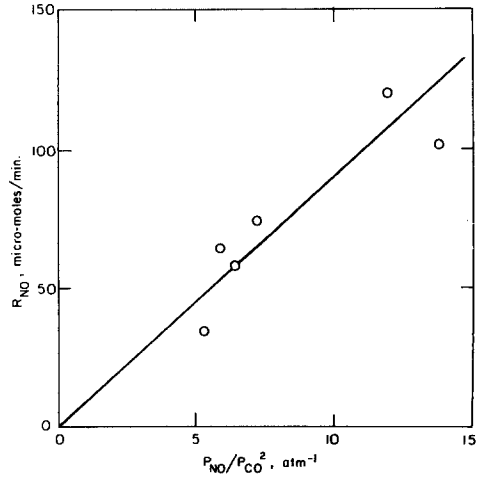


FIG. 12. Correlation of NO reduction rate with $P_{NO}/P_{CO}^2$ for reducing conditions.

of the best fitting straight line, the value of $k$ is found to be 5.63 molecules-atm/Pt site-sec. The average deviation of the data from the predicted rate is $\pm 17\%$. A similar analysis for data taken 180 min into a run gives a value of $k$, 76% smaller than that obtained at 60 min. In this case, the average deviation is $\pm 15\%$. One possible cause for the significant scatter observed in Fig. 12 is the influence of catalyst deactivation. By choosing data for a fixed reaction time it is implicitly assumed that the extent of deactivation is identical for different feed compositions. However, this assumption is not strictly valid.

To determine whether the proposed mechanism might describe the observed trends in $N_2O$ selectivity with gas composition, it is necessary to first obtain an expression for $r_{N_2}/r_{N_2O}$. Assuming that reaction 5a controls the formation of $N_2O$, $r_{N_2}/r_{N_2O}$ is given by the following expression:

$$r_{N_2}/r_{N_2O} = \frac{1}{2}\left[\left(1 + \frac{4k_4k_3}{k_{5a}^2K_2P_{NO}}\right)^{\frac{1}{2}} - 1\right]. \quad (5)$$

Equation (5) is then substituted into Eq. (1), which upon rearrangement gives

$$(2/S_{N_2O} - 1)^2 - 1 = \frac{4k_4k_3}{k_{5a}^2K_2} P_{NO}^{-1}. \quad (6)$$

A plot of the left-hand side of Eq. (6) versus the reciprocal of $P_{NO}$ is shown in Fig. 13. With the exception of a single point, the data fall along a straight line. On the other hand, if reaction 5b is taken as the primary path to $N_2O$, then Eq. (7) expresses the expected relationship between $N_2O$ selectivity and gas composition. A plot of the left-hand side

$$P_{NO}[(2/S_{N_2O} - 1)^2 - 1]^{-\frac{1}{2}} = \frac{k_{5b}}{4k_4k_3K_2}(1 + K_1P_{CO}) \quad (7)$$

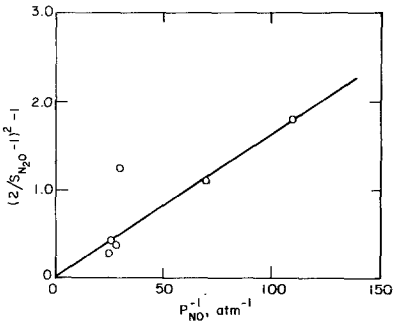


FIG. 13. Correlation of $N_2O$ selectivity with $1/P_{NO}$ for reducing conditions.

of Eq. (7) versus $P_{CO}$ does not correlate the data along a straight line. Based on this analysis, it is concluded that reaction 5a provides a more satisfactory description of $N_2O$ formation than reaction 5b, in agreement with the work of Cant *et al.* (*8*).

The kinetics obtained under oxidizing conditions cannot be interpreted properly because of the very high CO conversions achieved in this case. Nevertheless, it is possible to infer some qualitative differences between the mechanism operative under reducing and oxidizing conditions. To begin with, we observe that because of the high CO conversion under oxidizing conditions the partial pressure of CO in the reactor is small relative to that in the feed. Consistent with this, infrared spectra of the catalyst show that the Pt surface is no longer dominated by adsorbed CO. Since chemisorbed NO is not evident under oxidizing condition, it suggests that the balance of the surface is populated by nitrogen and oxygen atoms. In view of this, one would expect that the rate-limiting process now becomes the removal of these adsorbed atomic species. When the ratio CO/NO in the feed is only slightly less than unity it is not clear whether the removal of nitrogen or oxygen is rate limiting. However, when the ratio becomes significantly less than one, it seems reasonable to expect that the re-

TABLE 1

Accumulation of NCO Groups

| Feed concn (mole%) | | Integ. excess $CO_2$ ($\mu$mole) | Moles NCO/ mole surface Pt |
|---|---|---|---|
| NO | CO | | |
| 5.1 | 6.3 | 248 | 0.95 |
| 2.5 | 3.5 | 264 | 1.0 |
| 2.2 | 5.0 | 497 | 1.9 |
| 5.2 | 10.0 | 707 | 2.7 |
| 5.0 | 9.0 | 1280 | 4.9 |

moval of atomic oxygen by reaction 6 becomes rate limiting.

As was shown in Fig. 8, the $N_2O$ selectivity is essentially zero for a CO/NO ratio near unity and rises sharply as the CO/NO ratio decreases. This trend is consistent with the hypothesis that $N_2O$ is formed via the reaction of NO with adsorbed nitrogen atoms. However, whether $N_2O$ formation occurs through reaction 5a or 5b, cannot be deduced in this case.

*Catalyst Stability*

It will be recalled that under reducing conditions the catalyst exhibits a decline in NO reduction activity as well as in the production of $CO_2$ in excess of that required to balance the nitrogen-containing products. Concurrently, infrared spectra of the catalyst show the appearance of a strong NCO band and a weaker CN band, the growth of which does not affect the intensity of the CO band. Furthermore, the initial catalyst activity can be restored by either reductive or oxidative pretreatments and neither pretreatment affects the subsequent patterns of activity loss or growth of infrared bands. By contrast, under oxidizing conditions the catalyst does not deactivate, no excess $CO_2$ is formed, and the NCO band is weaker than under reducing conditions. The question now to be addressed is whether these observations provide a basis for explaining catalyst stability as a function of gas composition.

We begin by considering the connection between the formation of excess $CO_2$ and the accumulation of NCO groups on the silica support. The work of Voorhoeve *et al.* (*32*, *33*) and Solymosi *et al.* (*13*, *14*) clearly demonstrates that NCO is formed on the surface of the Pt crystallites. The nascent NCO groups do not appear to remain on the Pt surface but migrate rapidly to the support where they are stabilized as Si–NCO. This conclusion is supported by the observation that the position of the NCO band is in good agreement with the frequency for Si–NCO produced by decomposition of HCN (*24*), $C_2N_2$ (*24*), and $C_2H_5NCO$ (*23*) on $SiO_2$, and the fact that the NCO band position is virtually the same when NCO groups are produced by reaction of NO and CO over silica-supported Pt and Rh (*14*).

The oxygen atom associated with the nitrogen atom, which ultimately is stabilized as Si–NCO, reacts with CO to form $CO_2$, leading to the overall stoichiometry represented by reaction 7.

7. $Si + NO + 2CO \rightarrow Si\text{–}NCO + CO_2$

This reaction represents an additional pathway for $CO_2$ production and explains why the rate of $CO_2$ production under reducing conditions exceeds that required to stoichiometrically balance the formation of $N_2$ and $N_2O$. Based upon the data given in Figs. 1 and 5, it can be shown that not more than 10% and usually less than 5% of the total NO consumed is diverted to the formation of NCO groups. The amount of Si–NCO accumulated after 180 min of catalyst operation was estimated by integrating under the curves of excess $CO_2$ production versus time (Fig. 5). The results are listed in Table 1 and show that the accumulated NCO is equivalent to between one and five monolayers of Pt. These figures are comparable to those obtained by Solymosi *et al.* (*12*) in studies

of NCO formation over $Pt/Al_2O_3$. The fact that the NCO coverage can greatly exceed one Pt monolayer and the fact that NCO accumulation does not affect the intensity of the CO band associated with Pt–CO, further support the idea that NCO resides primarily on the support.

To accommodate the significant quantities of NCO observed on the support, the NCO groups must migrate from a Pt crystallite to fill in an area roughly two to three crystallite diameters in size (i.e., 30 to 50 Å). The mechanism of migration is not understood but may involve interaction with hydroxyl groups on the silica surface in a manner suggested by reaction 8.

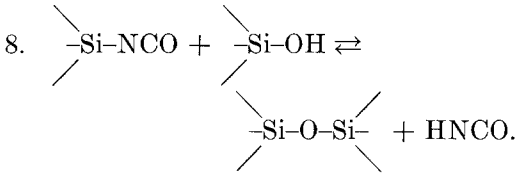


The generation of HNCO and its transport through the vapor phase could also explain the means by which NCO groups appear on the reference disk. While the forward direction of reaction 8 has not been reported, the reverse reaction has been used to produce NCO groups on silica (*14*) and is analogous to the decomposition of $C_2H_5NCO$ (*23*).

The appearance of a Si–CN band in the spectra of the catalyst is puzzling and cannot be explained easily. Such groups were observed by Eley *et al.* (*24*) when $C_2H_5NCO$ was decomposed on silica and were ascribed to the thermal decomposition of Si–NCO. It is possible that a similar mechanism is operative in the present case as well.

The close correlation between catalyst deactivation and the production of excess $CO_2$ suggests that the formation of NCO groups and their migration onto the support could be responsible for the loss in catalytic activity. Such an effect might result from the formation of electronegative patches on the support due to the accumulation of Si–NCO and Si–CN groups in the immediate vicinity of each Pt crystallite. In view of the very small size of the Pt crystallites (~14 Å) and their intimate contact with the support, a change in the local electronegativity of the support could result in a slight transfer of electronic charge from the metal crystallites to the support. A similar effect has been observed when metal particles are supported on oxides of differing electronegativity (*21*, *34*). As a consequence of charge transfer to the support, the availability of Pt valence electrons for interaction with an adsorbate should be reduced. Such an effect would be expected to inhibit the dissociation of NO, since this process is facilitated by the transfer of charge into the antibonding $\pi^*$ orbital of NO, and hence the rate of NO reduction. Since the formation of NCO groups also depends upon NO dissociation, a reduction in the dissociation rate should cause a reduction in the rate of NCO formation as well.

The proposed deactivation mechanism could also explain why deactivation was observed under reducing conditions, but not under oxidizing conditions. In the presence of excess NO the reduction rate was very rapid, leading to a very low partial pressure of CO over the catalyst surface. Such conditions would reduce the formation NCO groups (*11*), and hence explain the less intense NCO bands observed under oxidizing conditions (see Fig. 10). Because of the reduced rate of their formation NCO groups could migrate away from the Pt crystallites before large accumulations of Si–NCO could occur in the areas immediately adjacent to the crystallites. The net result would be to allow the catalyst activity to remain at its initial level. If on the other hand the accumulation of NCO species were to

become much larger, one would expect deactivation to occur even under oxidizing conditions. While this was not observed in the present studies, it was noted by Niiyama *et al.* (*16*) who carried out their investigation of NO reduction using CO/NO ratios of 0.33 to 0.67.

It should be noted that if the deactivation mechanism outlined above is correct, then the extent of charge transfer from the Pt crystallites to the support must be small. If it were not, then one would expect to see an upscale shift in the position of CO band due to a weakening in the Pt–C bond (*21*, *34*). The absence of an observable shift in the CO band position during the course of reaction may imply that the extent of charge transfer is sufficient to cause a change in the case of NO dissociation but not so large as to cause a change in the bonding of chemisorbed CO.

An alternative mechanism of deactivation involving NCO groups was proposed by Niiyama *et al.* (*16*). In their studies, using a $Pt/Al_2O_3$ catalyst, they observed a simultaneous reduction in NO conversion and the growth of an NCO band at 2250 $cm^{-1}$. The authors associated the appearance of the NCO band with the accumulation of NCO on the Pt surface and, hence, with a loss in active surface area. This interpretation, however, does not seem plausible and is inconsistent with several observations made in this investigation. To begin with the band observed at 2250 $cm^{-1}$ is very likely not due to Pt–NCO but rather to Al–NCO, as would be indicated by the work of Solymosi and Bánsági (*14*), Dalla Betta and Shelef (*15*), and Guillet *et al.* (*35*). Second, one would expect that if the Pt surface was to be covered by a significant concentration of NCO groups then this would reflect itself on the availability of sites for CO adsorption. Failure to see a decline in the CO band intensity with increasing NCO coverage suggests that a deactivation mechanism involving simply a loss in surface area is probably not valid.

Two additional deactivation mechanisms were also considered. The first is that the Pt becomes deactivated by gradual oxidation. Such a mechanism was proposed by Katzer (*36*) to explain the decline in activity of a $Pt/Al_2O_3$ catalyst used to reduce NO with $NH_3$. Stable Pt–O species have been reported by several investigators (*37–39*) and are known to inhibit the dissociation of NO (*27*, *40*). However, the fact that extensive preoxidation of the catalyst with NO did not influence the initial catalyst activity nor its pattern of deactivation (see Fig. 2), and the fact that the catalyst could be reactivated by oxidative pretreatment, make it highly unlikely that deactivation is caused by adsorbed oxygen.

Carbon formation on the surface of Pt was also examined as a possible cause for deactivation. This mechanism was prompted by the observation of Iwasawa *et al.* (*41*) that CO dissociation could occur at coordinately unsaturated sites on a Pt surface. Here again, though, the experimental data do not support the hypothesis. As was shown in Fig. 2 pretreatment of the catalyst in CO does not alter either the initial catalyst activity or the subsequent pattern of deactivation.

In summary, then, we believe that the interpretation of deactivation most consistent with all observations is the first one proposed, namely, that the catalytic properties of Pt crystallites are altered by the accumulation of large concentrations of NCO and CN groups on the support surface immediately adjacent to the crystallites. The recovery of activity after exposure of the catalyst to either an oxidizing or reducing atmosphere is also consistent with such a model of deactivation. In the absence of reaction, the production of NCO groups ceases and

those groups already present on the support can migrate away from the vicinity of the Pt crystallites. While the total accumulation of NCO groups, and hence the NCO band intensity, does not change, the concentration of NCO groups adjacent to Pt crystallites decreases, thereby restoring the original catalyst activity.

Finally, we note that the NCO groups present on the silica support are readily removed by reaction with $H_2O$. The ultimate products of this process are very likely $NH_3$ and $CO_2$ (*42*). While the mechanism of hydrolysis is not understood it is possible that CN groups are produced as intermediates, inasmuch as the growth of the CN band is observed during hydrolysis at 25°C (see Fig. 11).

## ACKNOWLEDGMENT

This work was supported by a grant (ENG76-20284) from the National Science Foundation.

## REFERENCES


1. Shelef, M., Otto, K., and Gandhi, H., *J. Catal.* **12**, 361 (1968).
2. Shelef, M., and Gandhi, H., *I&EC Prod. Res. Dev.* **11**, 393 (1972).
3. Shelef, M., and Kummer, J. T., *Chem. Eng. Prog. Symp. Ser.* **67**, 74 (1972).
4. Shelef, M., *Cat. Rev. Sci. Eng.* **11**, 1 (1975).
5. Bauerle, G. L., Service, G., and Nobe, K., *I&EC Prod. Res. Dev.* **11**, 54 (1972).
6. Kobylinski, T. P., and Taylor, B. W., *J. Catal.* **33**, 376 (1974).
7. Lambert, R. M., and Comrie, C. M., *Surf. Sci.* **46**, 61 (1974).
8. Cant, N. W., Hicks, P. C., and Lenon, B. S., School of Chemistry, Macquarie University, North Ryde, Australia, personal communication.
9. Unland, M. L., *Science* **179**, 567 (1973); *J. Phys. Chem.* **77**, 1952 (1973); *J. Catal.* **31**, 459 (1973).
10. Solymosi, F., and Kiss, J., *J. Chem. Soc. Commun.* 509 (1974); *J. Catal.* **41**, 202 (1975).
11. Solymosi, F., Sárkány, J., and Schauer, A., *J. Catal.* **46**, 297 (1977).
12. Solymosi, F., Kiss, J., and Sárkány, J., *in* "Proceedings of the 7th International Vacuum Congress and 3rd International Conference on Solid Surfaces" (R. Dobrozemsky *et al.*, Eds.). Vienna, 1977.
13. Solymosi, F., Völgyesi, L., and Sárkány, *J. Catal.* **54**, 336 (1978).
14. Solymosi, F., and Bánsági, T., "Infrared Spectroscopic Study of the Adsorption of Isocyanic Acid," to be published.
15. Dalla Betta, R. A., and Shelef, M., *J. Mol. Catal.* **1**, 431 (1976).
16. Niiyama, H., Tonaka, M., Iida, H., and Echigaya, E., *Bull. Chem. Soc. Japan* **49**, 207 (1976).
17. London, J., and Bell, A. T., *J. Catal.* **31**, 32 (1973).
18. Beck, A. F., Heine, M. A., Coule, E. J., and Pryor, M. J., *Corrosion Sci.* **7**, 1 (1967).
19. Boronin, V. S., Nikulina, V. S., and Poltarak, I. M., *Russ. J. Phys. Chem.* **37**, 626 (1963).
20. Benesi, H. A., Curtis, R. M., and Studer, H. P., *J. Catal.* **10**, 328 (1968).
21. Little, L. H., "Infrared Spectra of Adsorbed Species." Academic Press, New York, 1966.
22. Brown, M. F., and Gonzalez, R. D., *J. Catal.* **44**, 447 (1976).
23. Eley, D. D., Kiwanuka, G. M., and Rochester, C. M., *J. C. S. Faraday Trans. I* **69**, 2062 (1973).
24. Morrow, B. A., and Cody, I. A., *J. C. S. Faraday Trans. I* **71**, 1021 (1975).
25. Dunken, H., and Hobert, H., *Z. Chem.* **3**, 398 (1963).
26. Chang, C. C., and Hegedus, L. L., "Surface Reactions of NO, CO, and $O_2$ over Pt Near the Stoichiometric Point," presented at the 176th ACS National Meeting, Miami Beach, September 11–17, 1978.
27. Pirug, G., and Bonzel, H. P., *J. Catal.* **50**, 64 (1977).
28. Wilf, M., and Dawson, P. T., *Surf. Sci.* **60**, 561 (1976).
29. Schwaha, K., and Bechtold, E., *Surf. Sci.* **66**, 383 (1977).
30. Weinberg, W. H., and Merrill, R. P., *J. Catal.* **40**, 268 (1975).
31. Bonzel, H. P., and Ku, R., *J. Vac. Sci. Tech.* **9**, 663 (1972).
32. Voorhoeve, R. J. H., Trimble, L. E., and Freed, D. J., *Science* **200**, 759 (1978).
33. Voorhoeve, R. J. H., and Trimble, L. E., *J. Catal.* **53**, 251 (1978); **54**, 269 (1978).
34. Figueras, F., Gomez, R., and Primet, N., *Advan. Chem. Sci.* No. 121, 480 (1973).

*35.* Guillet, A., Condurier, M., and Donnet, J. B., *Bull. Soc. Chim. Fran.* **7–8**, 1563 (1975).
*36.* Katzer, J., *in* "Catalytic Chemistry of Nitric Oxides" (R. L. Klimisch and J. G. Larson, Eds.). Plenum Press, New York, 1975.
*37.* Lang, B., Joyner, R. W., and Somorjai, G. A., *Surf. Sci.* **30**, 454 (1972).
*38.* Gland, J. L., and Korchak, V. N., GM Research Labs Report PC-66, June 28, 1977.
*39.* Hopster, H., Obach, H., and Cosma, G., *J. Catal.* **46**, 37 (1977).
*40.* Amiranazmi, A., and Boudart, M., *J. Catal.* **39**, 383 (1975).
*41.* Iwasawa, Y., Mason, R., Textor, M., and Samorjai, G. A., *Chem. Phys. Lett.* **44**, 468 (1976).
*42.* Solymosi, F., and Sárkány, J., *Reac. Kinet. Catal. Lett.* **3**, 297 (1975).